JOURNAL OF PROPULSION AND POWER
Vol. 24, No. 3, May–June 2008

Low-Heat-Load-Vane Profile Optimization, Part 2: Short-Duration Shock-Tunnel Experiments

Jamie J. Johnson* and Paul I. King†
Air Force Institute of Technology,
Wright–Patterson Air Force Base, Ohio 45433
and
John P. Clark,‡ Michael J. Flanagan,§ and Ryan P. Lemaire¶
Air Force Institute of Technology,
Wright–Patterson Air Force Base, Ohio 45433

DOI: 10.2514/1.28501

Complete knowledge of the heat transfer over the surfaces of turbine components within their harsh operating environments is key to knowing the durability of a given airfoil design. Here, a nominal turbine inlet vane was tested for unsteady-heat-load measurements in a low-aspect-ratio linear cascade. A new airfoil called the low-heat-load vane, designed specifically for a reduced heat load, was tested experimentally and unsteady-heat-load trends were compared with the nominal vane counterpart. The tests were performed in a reflected-shock tunnel to validate the flow solver and turbomachinery design system used to generate the new airfoil shape, for which special attention was paid to leading-edge and suction-side heat-flux characteristics. Results indicate an appreciable reduction in heat load relative to the nominal vane. This work lends credibility to designing turbine airfoils for durability with the same emphasis normally given to designing for aeroperformance.

Nomenclature

A/A^*	=	area ratio
M	=	Mach number
P	=	pressure
q''	=	heat flux
Re	=	Reynolds number
T	=	temperature
Tu	=	freestream turbulence level
γ	=	ratio of specific heats

Subscripts

ex	=	exit
in	=	inlet
t	=	total flow property
2	=	exit condition
4	=	driver-section property
5	=	property behind reflected shock
θ	=	based on momentum thickness

Presented as Paper 3386 at the 9th AIAA/ASME Joint Thermophysics and Heat Transfer Conference, San Francisco, 5–8 June 2006; received 24 October 2006; revision received 20 November 2007; accepted for publication 20 November 2007.

*Captain, U.S. Air Force; Student, Department of Aeronautics and Astronautics, 2950 Hobson Way. Member AIAA.

†Professor, Department of Aeronautics and Astronautics, 2950 Hobson Way. Senior Member AIAA.

‡Senior Analyst, Turbine Branch, Propulsion Directorate, 1950 Fifth Street. Member AIAA.

§Senior Engineer, Turbine Branch, Propulsion Directorate, 1950 Fifth Street. Member AIAA.

¶Second Lieutenant, U.S. Air Force.

I. Introduction

UNDERSTANDING the characteristics of the boundary layer over the airfoil suction side (SS) and pressure side (PS) is essential to magnitude estimation of local heat transfer, given that the transition to turbulent boundary layers from the laminar type generally increases heat flux. Constant increased heat flux during engine operation reduces component durability, for example, in the form of excessive corrosion, cracking, or failure of thermal barrier coatings. The current work, originally reported in more detail as a thesis [1] and as a follow-up study to previous work [2], attempts to show that airfoil geometries designed for reduced heat transfer perform well in turbine-engine-representative conditions. Comparative physical performance of a nominal (nom) vane design and a new airfoil designed for improved thermal performance in a reflected-shock-tunnel cascade apparatus is accomplished. The new airfoil, called the low-heat-load (LHL) vane, was successfully designed for reduced leading-edge (LE) heat flux and delayed SS transition in part 1 [2] of this paper using a validated flow-solver code and a novel turbomachinery design system. From the conclusions drawn herein, turbine component designers can use heat-transfer-reduced designs to subsequently improve them with modern cooling techniques, realizing significant gains in component thermal performance, durability, and operating life, relative to current state-of-the-art designs.

Significant work has been conducted to examine the heat-transfer trends within the turbomachinery of airbreathing propulsion engines. Spatially resolved heat-flux findings in engine-representative conditions pioneered by Dunn and Stoddard [3] helped identify heat-transfer problem areas on turbine engine components. Some of the first experimental evidence of SS transition to turbulence was concluded from these experiments. A full turbine stage with shock-tube-generated flow later helped gathered stator and rotor data showing increasing heat transfer with increasing chord Reynolds number [4] and extended the transition results of [3]. Work done on the same rig as in the current work has showed that heat flux tends to be of the highest magnitude near the LE stagnation point and toward the trailing edge (TE) on the SS of vanes in a similar cascade [5]. Pressure-side heat flux was shown to be significantly less than with the suction-side data. Also, with increasing inlet Mach numbers, SS transition tended to toward the LE, increasing the length of transitional flow and increased heat flux.

A number of previous studies have attempted to predict heat-transfer data in turbine-engine-representative environments, with the goal of further validating existing codes. Turbulent flat-plate correlations and post-transition boundary-layer codes overpredicted surface heat-transfer data of [4], especially on the SS [6]. Predictions of light-piston-tunnel experiment data at varying turbulence levels Tu has also shown underprediction of the SS heat-transfer coefficient and a common lack of prediction of SS transition onset [7]. Simoneau and Simon [8] also noted this trend in a summary of flow prediction methods. Further work in predicting [3] data using a flow-solver code and an early turbine design system led to good agreement with rotor blade PS and SS heat transfer [9,10]. But later efforts to model rotor heat flux using two different codes showed underprediction of heat-transfer levels on the SS at three midspan locations and showed inaccuracy in predicting transition characteristics [11]. However, the PS data were predicted well, even using basic turbulent flat-plate theory. Historically, cascade PS characteristics have been easily simulated, perhaps because favorable pressure gradients accelerate flow, stabilizing the boundary layer, and counteracting the effects of freestream turbulence [12]. Flat-plate prediction of a low-aspect-ratio turbine stage led to more underprediction of heat-flux data on a vane surface with early transition to turbulence exhibited, whereas the rotor data were predicted with more accuracy [13]. This trend is also seen when two inviscid codes are used to predict the low-aspect-ratio turbine data and full-turbine-stage data of Dunn and Hause [4]. Here again, measured surface heat transfer exceeds theory [14]. More recent spanwise modeling of [4] rig data using two different state-of-the-art codes also underpredicted heat flux, except at the LE [15]. Clearly, heat-transfer levels on turbine components, especially on the suction side of inlet vanes, have been problematic to the point that a majority of work done to predict this trend has failed.

Studies done to predict turbine-inlet-flow heat transfer with varying levels of turbulence have shown dramatic increases in experimental heat flux with Tu, transition onset progression toward the LE with increasing Tu, little rotor heat-flux dependence on Tu, and more underprediction of PS and SS vane heat flux, especially at high Tu [16–18]. Boyle et al. [19] compared four transition models for predicting the Stanton number due to varied Tu with vane data compiled by multiple authors, including Radomsky and Thole [20] and Arts et al. [21], from a range of flow conditions. Prediction results of the Abu-Ghannam and Shaw transition-length model [22] is of primary interest because it was a critical part of the flow-solver code used in this effort. It predicted vane PS heat transfer well, is preferred for higher Reynolds number flows, uses a conservative length model, and it underpredicted SS heat transfer on some occasions. Trends in all of these cases indicate early transition from higher Tu and inlet Reynolds number and a general underprediction of SS heat transfer.

The preceding case studies present a compelling case for the need to further understand turbine nozzle guide vane leading-edge and suction-side heat-transfer characteristics and, through modern optimization algorithms, to create a high-thermal-performance vane with exceptionally lowered-heat-load qualities [2], which can be properly validated by both modern predictive and experimental methods. The current goal is to compare two turbine vane airfoil designs and observe a lower heat load in the optimized vane (LHL vane), designed using two types of optimization algorithms in part 1, by means of linear-cascade reflected-shock short-duration experiments. The enginelike flow conditions ($T_{t,\text{in}}$, M_{in}, Tu) are created in a shock-tube facility. It is anticipated that the following will be a step toward a modern solution to an old and pervasive problem in turbomachinery design, contributing to lower heat-flux designs and thus more accurate turbine vane heat-transfer prediction. This also may provide a basis for validation of optimization methods for reduced-heat-load operational vane designs.

II. Experimental Setup

Many different facilities have been used in the past to perform turbine-related heat-transfer studies. They may fall into two main categories: long-run-time (i.e. steady-state) facilities and those that have short run durations. Notable long-run-time facilities include those used by Blair et al. [16], Graziani et al. [23], and York [24], which tend to be more common in industry. Short-run-time facilities of distinction include the shock-tunnel facility used extensively by Dunn and Hause [4] and the isentropic-light-piston tunnel (ILPT) employed by Nicholson et al. [29]. The apparatus used here falls into the latter category, along the lines of the facilities used by Dunn and Hause [4], because short-duration methods use much less power, are less expensive to operate, and are regularly much more convenient and repeatable than long-run-time flow facilities. In addition, as seen by the preceding works, short-run-time facilities have long been established as a validated technique for performing aerodynamic and heat-transfer measurements.

For the experiment at hand, a rectangular-cross-section, low-driver/driven-pressure-ratio shock tube used in past thesis experiments [5] was used to model the high-temperature, high-pressure environment of a turbine inlet to measure heat transfer on the nominal and optimized vanes in a turbine-representative environment. The shock tube consists of a high-pressure driver section and a relatively low-pressure driven section separated by a diaphragm. The driver section was pumped up to a desired pressure while the driven side was evacuated to a desired pressure to increase the magnitude of shock pressure ratio. In the current experiment, only the driver-side pressure was increased and the driven side was kept at atmospheric pressure. Using well-established transient test techniques, the shock tube can be used to obtain spatially resolved heat-transfer rates on different gas-turbine components. The shock tube is a total of 4.88 m (16 ft) in length with a 1.22-m (4-ft) driver section, a 3.66-m (12-ft) driven section, and a uniform rectangular internal cross section of 10.15 cm (4 in.) by 20.32 cm (8 in.). A 0.83-MPa (120-psi) compressor air supply system was used to increase and control the driver-side pressure. The driver section lies on a two-axis mobile platform for ease of repeatability of experimental runs in replacing diaphragms and removing used diaphragm fragments. Once a proper diaphragm is installed, the driver and driven sections are held together with a hydraulic clamp built onto the driven section and operated using a hand pump. Mylar sheets of varying thickness are available for use in the shock tube as diaphragms to separate the two sections. For the purposes of this effort, the diaphragms used were 1.78×10^{-4} m (0.007 in.) thick and installed with thin rubber gaskets on both sides between the clamped sections to help prevent air leakage. The diaphragm was ruptured and the shock initiated using a nonintrusive hand-trigger-operated pneumatic spike built into the center of the driver section. The shock tube was connected to the vane cascade test section at the end of the driven section.

The test section used in the current experiment made it possible to take heat-transfer data at midspan for both the nom vane and the vane optimally designed in this study: the LHL vane. The linear cascade consisted of seven airfoils mounted with a 0-deg inlet flow angle, in which only the fourth airfoil for each of the vane geometries was instrumented for heat-flux assessment. The vanes were separated by a pitch of 3.378 cm (1.33 in.), creating six passages between vanes, and good flow periodicity was provided, in that data were only taken on the middle of the seven vanes. The solidity is 0.64 and pitch-to-chord ratio is 1.56. The original nozzle guide vane tested by Arts et al. [21] had an axial chord of 4.178 cm (1.645 in.). The vanes tested in the shock-tube cascade are approximately half-scale (52%), having an axial chord of 2.178 cm (0.8575 in.), which results in a relatively low aspect ratio of 1.166. The chord value was used in the numerical portion of this work for both the nom and LHL vanes and kept constant as a main control to simplify the optimization of the vane and reduce complexities due to the necessity of different turbine stage axial dimensions caused by larger or smaller axial chord lengths. High freestream turbulence conditions were simulated with the insertion of a turbulence grid upstream of the test section designed for 6% Tu. The grid was removed for low-Tu experimental conditions. It should be noted that although the pressure and temperature entering the cascade test section provide realistic nondimensional flow parameters, the flow in the experiment is atmospheric air and not combustion products as in the real environment of a turbine engine inlet.

Table 1 Comparison of nom and LHL vane details with modern nozzle guide vanes

Vane details	Military SOA	HIT TR	NOM	LHL
Exit Mach number	0.82	0.89	0.80	0.80
Pitch/axial chord	1.39	1.91	1.56	1.56
Zweifel coefficient	0.73	0.85	0.79	0.77
Turning, deg	75	78	75	75

The cascade vanes were chosen to be comparable with typical turbine engine flow conditions. Table 1 shows that both vanes being tested experimentally have exit Mach numbers consistent with modern high reaction turbines. In addition, their pitch-to-chord ratios and Zweifel coefficients are larger than state-of-the-art military turbines (e.g., the F119). So, because the vanes happen to show evidence of typical aerodynamic qualities they are a suitable step in the direction of the high-impact turbine (HIT) turbine rig (TR), which is itself a representative turbine for future long-range strike aircraft.

Seven identical acrylonitrile butadiene styrene (ABS) plastic vanes coated with a very thin layer of copper 381 μm (1.5 mil) thick to reduce surface roughness made up the linear cascade situated between two 1.9-cm (3/4-in.) clear Plexiglas walls that were screwed together by an aluminum framework on the outside. The copper layer was added to give all the vanes smoother surfaces than if they had the rough plastic finish as seen just after fabrication, but no validation was done to ensure engine-representative surface roughness was achieved. It was decided that because the layer of copper was so thin relative to the thickness of the vanes, that the plastic vane thicknesses did not have to be reduced to accommodate the copper thickness. The inlet and outlet areas were 12.9 and 51.6 cm^2 (2 and 8 in.^{2}), respectively, thus the throat of the test section is at its exit. The cascade lies 2.54 cm (1 in.) downstream of the test-section inlet. Both sets of vanes had the same value of flow turning as well, about 75 deg, just as they did for their CFD analyses. The inlet Mach number upstream of the cascade row can be estimated from the known test-section area ratio, $A/A^* = 4$. From isentropic relation tables for air (assuming $\gamma = 1.4$) this critical area ratio corresponds to an inlet Mach number M of about 0.15 and an inlet static to total pressure ratio, P_{in}/P_t, of about 0.98. From this P_t can be found and knowing that the exit static to total pressure ratio is found by $P_{\text{ex}}/P_t = P_{\text{ex}}/P_{\text{in}} \times P_{\text{in}}/P_t$, the exit isentropic Mach numbers are found to be between about 0.80 and 0.85 for most runs. This value is comparable with the vane exit Mach numbers seen in Table 1 by designers of a future research turbine (HIT TR) and by Dunn et al. [10] and Arts et al. [21]. The test-section Plexiglas walls held the vanes in place by compression using metal pins, three per vane, and these lie in a pattern such that both the nom and LHL vanes were interchangeable for testing at any time. Because this is a small-aspect-ratio cascade, there is good reason to believe that secondary flow effects could hinder quality heat-flux data at midspan. A detailed analysis of the 3-D vane flowfield in the test section using CFD tools and recent empirical prediction techniques from open literature show that the aspect ratio and turning value for the vanes are acceptable for assessing midspan heat flux. The examination revealed that horseshoe vortices generated due to endwall secondary flow only propagates to 15% span on each end of the vane at the trailing edge, suggesting that it is safe to monitor flow properties such as heat flux at 50% span.

Figure 1 is a schematic of the shock-tube linear-cascade test section and its main features, with the airflow going from right to left. The static pressure tap arrays upstream and downstream of the vane row in the Plexiglas endwall were essential in calculating Mach numbers for each run. The two other instrumentation ports positioned on the opposite Plexiglas endwall were used for probes to record total temperature T_t and total pressure P_t. These same ports were also used to measure Tu and length scales using a hot-wire anemometer probe to test the grid and make comparisons with the grid design Tu. No dump tank was attached to the end of the test section as in previous works using the shock tube, because there was

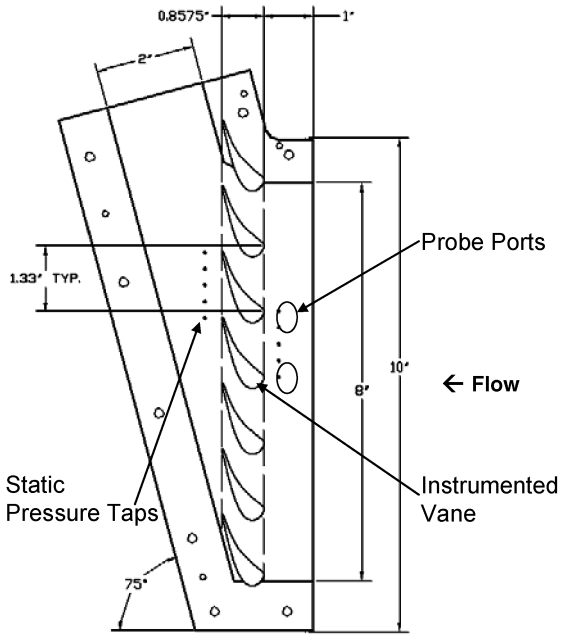

Fig. 1 Diagram of the shock-tube linear-cascade test section (shown with nom vanes installed).

no need to add one and the flow through the shock tube exited to atmosphere.

High-density thin-film heat-flux gauges [25] were used to obtain heat-transfer data at the midspan of each middle vane in the cascade to compare the nom with the LHL vane in the turbine-representative shock-tube test-section environment. The gauges designed specifically for this experiment are fundamentally similar to those used by Dunn et al. [13] and others in the past, in that voltage changes are measured across a thin-film resistance under constant current. However, the high-density-array gauges used here follow the design methods of Anthony et al. [26] and they have many advantages over older-technology gauges. These flexible films are virtually nonintrusive to the flow lying flush on the curved surface of the vanes. The gauges are composed of a thin flexible Kapton insulating substrate layer that is 50 μm thick with known thermal properties underneath a thin layer of conducting platinum metal that is 500 Å thick. They are also custom-designed for every new experimental application, as was the case here. The films were carefully adhered to the middle (vane 4) nom and LHL vanes in each cascade using an adhesive that was 50 μm thick. The platinum thin films with substrate are designed very thin so that they may be applied to any surface to make measurements; thus, the instrumented vane in the middle of the test-section vane row was not reduced or undercut to accommodate the small thickness of the films. Further details on the fundamental operation of the films are given in [1].

The nom and LHL vanes had a total of 27 and 28 midspan thin-film gauges, respectively, because the LHL vane had a slightly larger surface distance. The nom vane had 10 gauges on the PS and 17 on the SS, and the LHL vane had 10 gauges on the PS and 18 on the SS. The sizes of each gauge are consistent with good design practice, meeting the minimum 10:1 length-to-width ratio recommended for accurate data collection [25]. Finally, to investigate the heat transfer around the airfoil (because the focus areas for this study, as described before were reduced LE heat load and delayed transition), the gauge densities were increased (and the gauge sizes were decreased to the minimum possible size) near the leading edge and past approximately 50% of the suction surface for each vane. This provided increased data resolution around the surface in the areas of interest. There were two different gauge sizes on the thin films, in which the small gauges measured 0.2 by 2.0 mm and large gauges were 0.4 by 4.0 mm. As a result, large gauges had four times the area of the small gauges and, as a fundamental design requirement, the aspect ratio for all gauges was subsequently kept constant. All

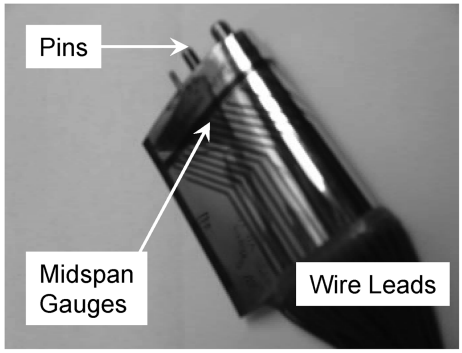

Fig. 2 Thin-film heat-flux gauges mounted on surface of nom vane.

gauges were spaced 0.2 mm apart. Figure 2 shows the fully instrumented nom vane.

Two high-sensitivity, fast-response, model XCS-062 Kulite pressure transducers rated to 1.034 MPa (150 psia) were used in the shock-tube sections to record absolute pressure. One was located in the driver section of the shock tube and the other was located toward the end of the driven section. The pressure transducer in the driver section gave real-time readings, and so it was known when the desired driver pressure was reached before the diaphragm was broken. The driven-section transducer was close to the test section and recorded wave-disturbance histories and pressures to help determine wave-reflection times and local flow properties. Model PDCR-22 Druck differential pressure transducers rated to 1.034 MPa (150 psid) were used to record static pressures in the test section in the form of two vertical five-hole arrays in the Plexiglas endwall that spanned one pitch length of 3.378 cm (1.33 in.), with one 0.635 cm (÷ in.) upstream and one 0.635 cm downstream, and that were centered on the flowpath between the instrumented vane and the vane above it in the cascade. Experimental inlet and exit isentropic Mach numbers were calculated with these data for each run. Total pressure data were taken in one of the probe ports using a pitot tube connected to a short pressure line that in turn was linked to another Druck pressure transducer. Special care was taken to keep the length of all pressure lines as short as possible to minimize pressure-reading lag; none of the lines were more than about 4 in. Heat-flux data were sampled at 200 kHz per channel and the pressure data were sampled at 10 kHz. The fully instrumented cascade test section from the heat-flux-gauge lead-wire side is shown in Fig. 3. Static pressure leads

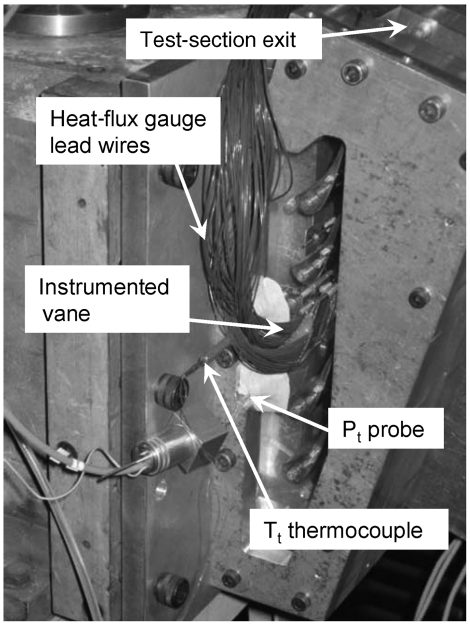

Fig. 3 Instrumented cascade test section positioned at the end of the shock tube.

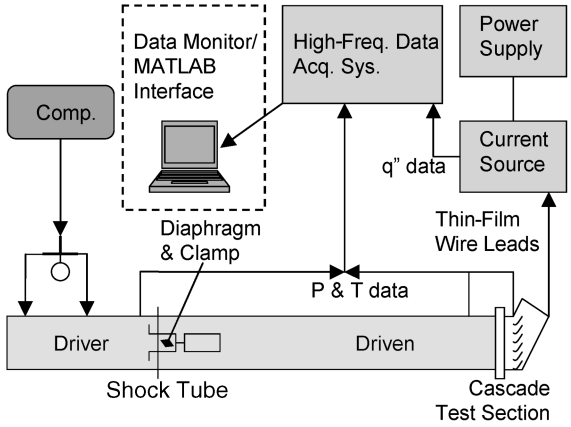

Fig. 4 Shock-tube cascade experimental setup.

came out the other side of the test section. In summary, a total of 9 Drucks, 2 Kulites, 1 thermocouple, and 27 (nom vane) or 28 (LHL vane) platinum thin films were used to obtain the essential data for each run. All the data were processed through a high-frequency data acquisition system. Figure 4 shows the basic experimental setup for the shock-tube experiment to investigate midspan heat transfer on both the nom and LHL vanes.

Uncertainties in the measurement of the midspan heat flux using the platinum thin-film gauges is expected to be on the order of $\pm 10\%$, as shown in a number of studies of heat-flux uncertainty using the same instruments [27,28]. Concerning pressure data error, the Kulite transducer error in the shock tube was $\pm 0.45\%$ of full scale. The Druck transducers used in the test section had uncertainties of approximately $\pm 0.2\%$ of full scale.

III. Results and Discussion

Before each shock-tube run, the current source boxes were given time to achieve a steady thermal state. A constant current of 4 mA was passed through the gauges. A Mylar diaphragm was installed and hydraulically clamped between the shock-tube driver and driven sections. Using a large compressor, the driver section of the tube was pumped to the desired pressure using the real-time readout of the driver-side Kulite transducer. A valve was used to seal the driver section and another valve was opened to release high-pressure air into the line for the spike piston. Ambient temperature and pressure were recorded. Driver pressure was monitored using laboratory software, and the sampling frequency and data buffer values could be entered, along with the desired test time. When the desired driver pressure was reached, the Mylar diaphragm was broken, sending a normal shock wave propagating down the tube. Data were collected for 2.5 s and written to a file for all runs. Observing the raw voltages traces, the average test times were on the order of 5 ms. Figure 5 shows the pitot pressure trace, along with Kulite traces, and the available test time from which to gather heat-flux data. The apparent line thicknesses account for measurement uncertainty. To repeat the process, the old Mylar diaphragm was taken out and discarded, the inside of the tube was inspected for debris, and a new diaphragm was installed. Heat-transfer data were reduced using the methods of Oldfield [29], consistent with a semi-infinite substrate thin-film heat-flux gauge. Codes created by Oldfield were used to deboost, filter, and convert raw voltage data to heat flux.

Because the tests only used one turbulence grid, the cascade experiments in the shock tube only examined two different values of Tu. Experimental turbulence was measured with a TSI 1210 T1.5 hot-wire probe and an IFA-300 constant-temperature anemometer that found levels of $5 \pm 1\%$ with the turbulence grid in and levels of $2 \pm 0.3\%$ without the grid. These values include a margin of error as prescribed by Mee and Dickens [30]. The experiments were run at one nominal inlet Reynolds number in which a single driver pressure of approximately 0.412 MPa (60 psia) was used for all runs. Thus, four runs of the nom and LHL vanes with the grid in and out were

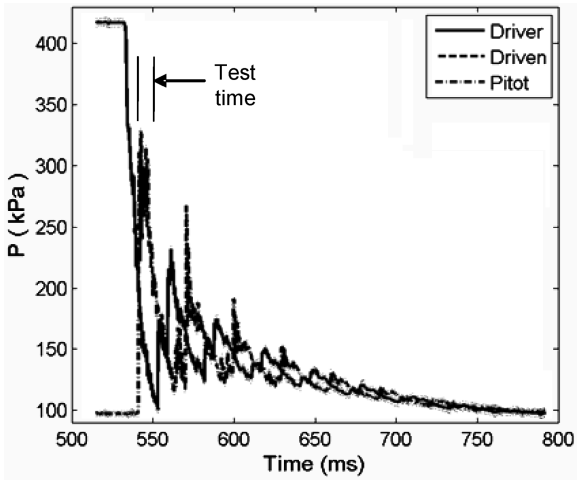

Fig. 5 Pressure histories for a sample shock-tube run with the test times denoted.

selected for heat-transfer analysis. Table 2 gives all run conditions and measured flow properties such as pressures and Mach numbers from the four runs for which heat-transfer data will be analyzed.

Figure 6a compares midspan heat-flux data with error bars from run numbers 10 and 11 for the nom vane with grid in and grid out. The pressure-side data are on the left half of the plots and the suction-side data are on the right, with the leading edge at the center. It is expected that this plot would show lower heat transfer for a case with no grid relative to a case with the turbulence grid for the same vane, which is seen for the most part, primarily for the high-magnitude heat-flux characteristics. Near the LE, there appears to be early transition followed by relaminarization. Near the TE, seeing a PS transition to such high heat flux is a surprise, knowing the typical historical data in open literature for similar Arts et al. [21] run conditions of M_2 and Re_2. The source of the high heat flux toward the TE is unknown at this point or the data are spurious. Both surfaces appear to show a rather sudden increase transition to turbulence after passing the LE and an area of extremely high heat transfer relative to the rest of the surface, especially on the SS, which is likely attributable to relaminarization with subsequent transition at about 60% of the fractional distance. The grid-out (lower-Tu) run appears to transition later, with overall lower heat-flux magnitudes, which agrees with expectations. Gauge 16 on the nom vane SS turned out to be faulty, as seen by its reading of zero heat flux. No comparisons of the nom vane data with that in the Arts et al. [21] data are made here, because the focus of the current work is to note relative heat-transfer characteristics between the nom and LHL vanes.

Data from the LHL vane grid-in and grid-out runs in Fig. 6b show that heat flux is much better behaved, compared with the data for the nom vane, especially on the PS. The distribution is smooth, with transition from a laminar boundary layer to a turbulent boundary layer at about 30% of the PS, although the entire PS may be laminar with higher levels of turbulence. Immediate transition occurs on the SS at about 4% of the surface distance. Interestingly, each vane

Table 2 Shock-tube experimental run conditions for vane midspan heat-transfer measurements

Run no.	10	11	16	17
Vane	NOM	NOM	LHL	LHL
Grid in?	Yes	No	Yes	No
P_4, MPa	0.42	0.41	0.42	0.41
P_5, MPa	0.27	0.28	0.28	0.27
$P_{t,\text{in}}$, MPa	0.27	0.28	0.28	0.27
$P_{s,\text{in}}$, MPa	0.26	0.27	0.27	0.26
$P_{s,\text{ex}}$, MPa	0.17	0.18	0.18	0.18
P_{amb}, MPa	0.10	0.10	0.10	0.10
M_{in}	0.216	0.208	0.188	0.211
M_{ex}	0.838	0.842	0.815	0.819

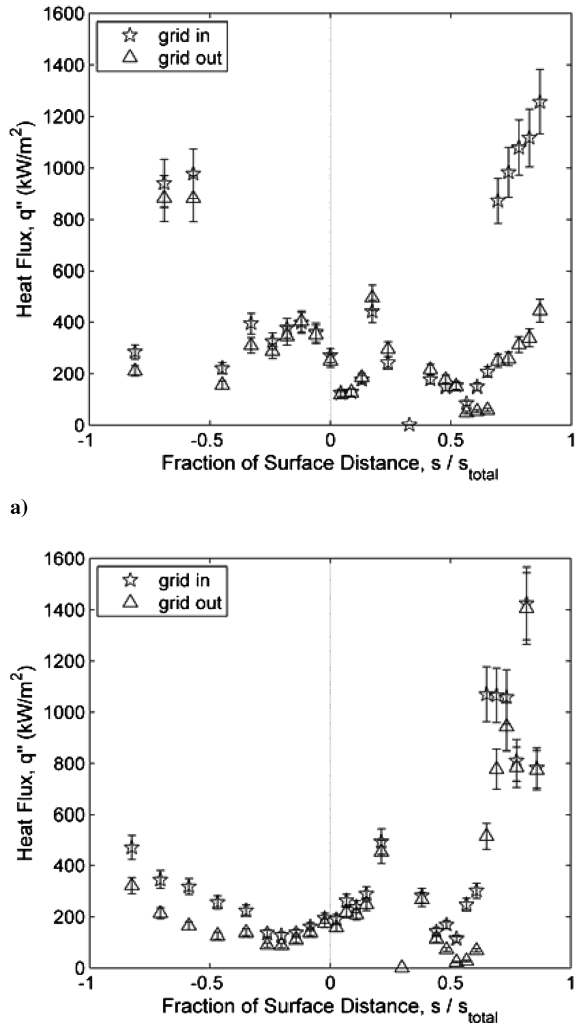

Fig. 6 Grid-in and grid-out heat-flux comparisons for the a) nom vane and b) LHL vane.

experienced early SS transition at the same fraction of surface distance, regardless of the level of Tu. More investigation may be necessary to explain this phenomenon, because historically, in numerous experiments, increasing Tu had caused earlier transition onset. The heat transfer from transition to turbulence on the SS is much more pronounced than that of the PS. The experimental SS boundary layer follows theory, because the heat transfer is high at first and decreases as the boundary layer grows. The SS heat transfer decreases so much, suggesting a relaminarization of the boundary layer, which may be possible, because the LHL vane was designed to delay transition as long as possible. The change in loading seen in the previous design work [2] supports this. Again, this second transition event occurs closer to the TE for the grid-out lower-Tu case, as it should.

The heat-transfer trends of the nom and LHL vanes are compared in Figs. 7a and 7b. Again, the pressure-side data are on the left half of the plot and the suction-side data are on the right, with the leading edge at the center. Figure 7a compares shock-tube grid-in experimental runs 10 and 16. These are the same data sets shown in Fig. 6, just compared differently. The LHL vane clearly exhibits significantly lower PS and lower LE heat transfer by almost 30% of the nom vane magnitude on the PS at the LE. This shows that the Wildcat code used in part 1 [2] of this paper, along with a turbine design system that used two types of algorithms, successfully designed the LHL vane for lower LE heat transfer relative to the nom vane [2]. The code used in the previous effort was a quasi-three-dimensional viscous fluid dynamics analysis tool for axial flow

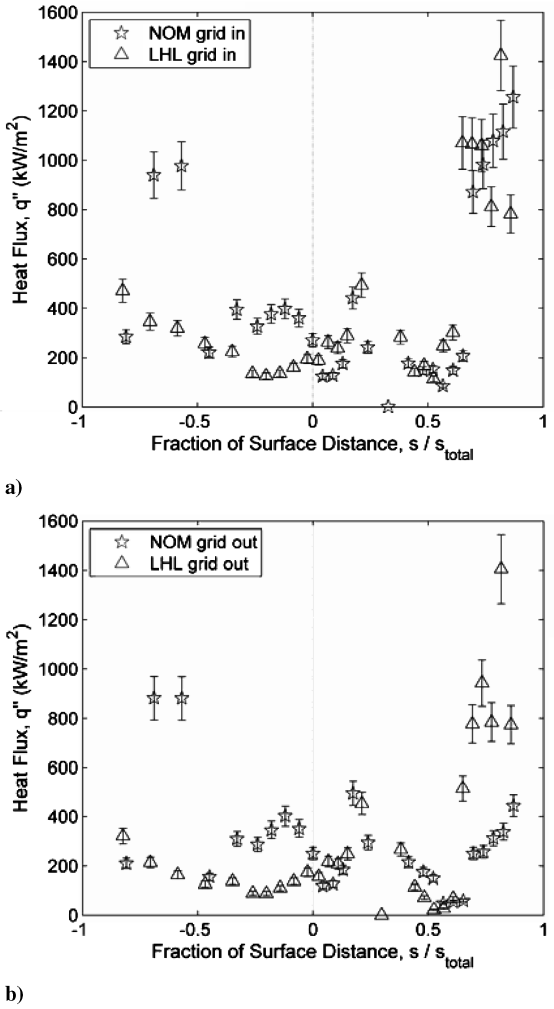

Fig. 7 Direct comparison of nom and LHL vane midspan heat flux for a) $Tu = 5\%$ and b) $Tu = 2\%$.

turbomachinery vane and blade rows by Dorney [31] named Wildcat [6] and has the ability to predict steady or unsteady flowfields for single or multiple blade rows and to generate grids. These Reynolds-averaged Navier–Stokes calculations with selected transition and turbulence models were embedded in an easy-to-use programming-based software turbine design and analysis system used by many turbine component designers and created by Clark [32].

Generally, the LHL vane is mostly laminar, with high heat transfer due to thinned-out boundary layers. Close inspection of the figure reveals that transition occurred at 11% of the SS distance for the LHL vane and at 4% for the nom vane. It appears for the LHL vane on the SS near the LE that there is a short-lived laminar boundary layer followed by transition to turbulence, whereas the nom SS LE data appear to immediately rise to turbulent levels of heat transfer, slightly lower than that for the LHL vane. Again, though, it is obvious that something currently unexplainable is causing excessive heat-transfer levels toward the TE. In addition, because both vanes essentially have immediate transition to turbulence, and with the positions of transition onset being so close with this unexplainably augmented heat transfer, it may not be appropriate to compare SS transition with these particular data. A discussion and brief analysis of the excessive heat transfer seen in Figs. 6 and 7 is given in later work, which suggests that the short test times in the current experiments caused underdeveloped boundary-layer flows [33]. Longer test times may be necessary to assess the heat-flux differences between the vane designs in this work. Finally, a root-mean-square calculation of the measured PS heat flux in Fig. 7a, a technique originally employed by Owen [34], exaggerated the dominant features in the midspan spatial distribution and showed a 25% delay in PS transition by the LHL vane.

The grid-out cases in Fig. 7b for the LHL vane show more favorable traits than in the case for higher freestream turbulence levels. On both surfaces, the LHL has generally lower heat transfer, with an apparent reduction in LE heat flux of over 30% compared with the nom vane, which is a larger reduction than in the design plots, which exhibited a 15% reduction. The only exception is the heat transfer near the TE, which is obviously more pronounced on the LHL vane SS. The reason for this occurrence suggests that more experimental investigation is necessary. However, the pressure-loading plots and predicted heat transfer for both vanes at these conditions gave no indication of shocks that would originate so far back from the TE; therefore, it may again be more likely that there is relaminarization followed by transition to higher levels of heat transfer.

The shock tube proved to be an inexpensive and highly repeatable rig for examining heat transfer on the nom and LHL vanes to find that the LHL vane exhibited generally lower heat flux, especially at the leading edge. One of the two goals that were established for obtaining a heat-load-optimized vane was met when it came to the experimental data. An additional benefit may be seen in the lower PS heat flux, due to delayed transition due to the loading. Table 3 is a review of the experimental heat-transfer attributes pertaining to the LE and SS transitions of the vanes. Values in the last three columns of the table were found upon closer examination of the data and noting the location of positive slope change. With the current resolution, these values are merely approximate. However, the present experimental measurements demonstrate the success of the design optimization in achieving lower heat transfer at the vane leading edge.

IV. Conclusions

A number of findings were made as a result of this follow-up study concerning experimental assessment of turbine component heat transfer of an airfoil designed specifically for reduced heat transfer using a novel turbomachinery design system and a validated flow-solver code [2]. Reflected-shock short-duration tests in a linear-cascade experiment allowed experimental comparisons of the nom and LHL vanes with and without a turbulence grid installed at similarity conditions that were consistent with a turbine inlet. Transient, spatially resolved, unsteady heat flux was measured at midspan. The low-heat-load (LHL) vane exhibited LE heat-transfer levels 28% lower than the nom vane for an estimated 5% Tu and 31% lower for 2% Tu. The LHL vane delayed PS transition 25% relative to the nom vane. However, the estimated early transition followed by relaminarization that was experienced on the SS of both vanes and the subsequent transition to turbulence near the trailing edge show that delaying transition on the SS was not achieved at this time by the LHL vane and perhaps requires additional experimental study.

Table 3 Summary of experimental heat-transfer characteristics for the nom and LHL vanes.

Vane	Approx. Tu, %	LE heat flux, kW/m^2	SS trans. onset, % SS	Second trans. location, % SS	PS trans. onset, %
NOM	2.0	270.93	4	57	45
NOM	5.0	250.33	4	57	10
LHL	2.0	194.21	11	53	None
LHL	5.0	173.87	11	53	35

Acknowledgments

The authors would like to acknowledge the contributions of R. J. Anthony and M. Ooten for their technical support on this effort. Additional support from individuals from the U.S. Air Force Research Laboratory and the Air Force Institute of Technology are also greatly appreciated.

References

[1] Johnson J, J., "Optimization of a Low Heat Load Turbine Nozzle Guide Vane," M.S. Thesis, School of Engineering, Air Force Inst. of Technology, Wright–Patterson AFB, OH, Mar. 2006.

[2] Johnson, J. J., King, P. I., and Clark, J. P., "Low-Heat-Load-Vane Profile Optimization, Part 1: Code Validation and Airfoil Redesign," *Journal of Propulsion and Power*, Vol. 24, No. 3, 2008, pp. 395–402. doi:10.2514/1.28530

[3] Dunn, M. G., and Stoddard, F. J., *Studies of Heat Transfer to Gas Turbine Components*, Calspan Corp., Buffalo, NY, 1977, pp. 1–48.

[4] Dunn, M. G., and Hause, A., "Measurement of Heat Flux and Pressure in a Turbine Stage," *Journal of Engineering for Power*, Vol. 104, Jan. 1982, pp. 215–223.

[5] Elrod, W. C., Gochenaur, J. E., Hitchcock, J. E., and Rivir, R. B., "Investigation of Transient Technique for Turbine Vane Heat Transfer Using A Shock Tube," *Proceedings of the Beijing International Gas Turbine Symposium*, Sept. 1985, pp. 1–10.

[6] Wistanley, D. K., Booth, T. C., and Dunn, M. G., "The Predictability of Turbine Vane Convection Heat Transfer," AIAA Paper 81-1435, 1981.

[7] Consigny, H., and Richards, B. E., "Short Duration Measurements of Heat-Transfer Rate to a Gas Turbine Rotor Blade," *Journal of Engineering for Power*, Vol. 104, July 1982, pp. 542–551.

[8] Simoneau, R. J., and Simon, F. F., "Progress Towards Understanding and Predicting Heat Transfer in the Turbine Gas Path," *International Journal of Heat and Fluid Flow*, Vol. 14, No. 2, June 1993, pp. 106–128. doi:10.1016/0142-727X(93)90019-J

[9] Dunn, M. G., Rae, W. J., and Holt, J. L., "Measurement and Analysis of Heat Flux Data in a Turbine Stage, Part 1: Description of Experimental Apparatus and Data Analysis," *Journal of Engineering for Gas Turbines and Power*, Vol. 106, Jan. 1984, pp. 229–233.

[10] Dunn, M. G., Rae, W. J., and Holt, J. L., "Measurement and Analysis of Heat Flux Data in a Turbine Stage, Part 2: Discussion of Results and Comparison with Predictions," *Journal of Engineering for Gas Turbines and Power*, Vol. 106, Jan. 1984, pp. 234–240.

[11] Dunn, M. G., "Heat-Flux Measurements for the Rotor of a Full-Stage Turbine, Part 1: Time-Averaged Results," *Journal of Turbomachinery*, Vol. 108, July 1986, pp. 90–97.

[12] Blair, M. F., "Influence of Free-Stream Turbulence on Boundary Layer Transition in Favorable Pressure Gradients," *Journal of Engineering for Power*, Vol. 104, Oct. 1984, pp. 743–750.

[13] Dunn, M. G., Martin, H. L., and Stanek, M. J., "Heat-Flux and Pressure Measurements and Comparison with Prediction for a Low-Aspect-Ratio Turbine Stage," *Journal of Turbomachinery*, Vol. 108, July 1986, pp. 108–115.

[14] Rae, W. J., Taulbee, K. C., and Dunn, M. G., "Turbine-Stage Heat Transfer: Comparison of Short-Duration Measurements with State of the Art Prediction," AIAA Paper 86-1465, 1986.

[15] Haldemann, C. W., and Dunn, M. G., "Heat Transfer Measurements and Predictions for the Vane and Blade of a Rotating High-Pressure Turbine Stage," American Society of Mechanical Engineers Paper GT2003-38726, 2003.

[16] Blair, M. F., Dring, R. P., and Joslyn, H. D., "The Effects of Turbulence and Stator/Rotor Interactions on Turbine Heat Transfer, Part 2: Effects of Reynolds Number and Incidence," *Journal of Turbomachinery*, Vol. 111, June 1988, pp. 97–103.

[17] Galassi, L., King, P. I., and Elrod, W. C., "Effects on Inlet Turbulence Scale on Blade Surface Heat Transfer," AIAA Paper 90-2264, 1990.

[18] Giel, P. W., Van Fossen, G. J., Boyle, R. J., Thurman, D. R., and Civinskas, K. C., "Blade Heat Transfer Measurements and Predictions in a Transonic Turbine Cascade," NASA TM 1999-209296, 1999.

[19] Boyle, R. J., Ames, F. E., and Giel, P. W., "Predictions for the Effects of Freestream Turbulence on Turbine Blade Heat Transfer," American Society of Mechanical Engineers Paper GT2004-54332.

[20] Radomsky, R. W., and Thole, K. A., "Detailed Boundary Layer Measurements on a Turbine Stator Vane at Elevated Freestream Turbulence Levels," American Society of Mechanical Engineers Paper 2001-GT-0169.

[21] Arts, T., Lambert de Rouvroit, L., and Rutherford, A. W., "Aero-Thermal Investigation of a Highly Loaded Transonic Linear Turbine Guide Vane Cascade," Technical Note 174, von Kármán Inst. for Fluid Dynamics, Rhode-Saint-Genèse, Belgium, Sept. 1990..

[22] Abu-Ghannam, B. J., and Shaw, R., "Natural Transition of Boundary Layers—The Effects of Turbulence Pressure Gradient and Flow History," *Journal of Mechanical Engineering Science*, Vol. 12, No. 5, 1980, pp. 1–18.

[23] Graziani, R. A., Blair, M. F., Taylor, J. R., and Mayle, R. E., "An Experimental Study of Endwall and Airfoil Surface Heat Transfer in a Large Scale Turbine Blade Cascade," *Journal of Engineering for Power*, Vol. 102, Apr. 1980, pp. 257–267.

[24] York, R. E., "Experimental Investigation of Endwall Heat Transfer and Aerodynamics in a Linear Vane Cascade," *Journal of Engineering for Gas Turbines and Power*, Vol. 106, Jan. 1984, pp. 159–167.

[25] Anthony, R. J., Jones, T. V., and LaGraff, J. E., "High Frequency Surface Heat Flux Imaging of Bypass Transition," *Journal of Turbomachinery*, Vol. 127, 2005, pp. 241–250. doi:10.1115/1.1860379

[26] Anthony, R. J., Oldfield, M. L. G., Jones, T. V., and LaGraff, J. E., "Development of High Density Arrays of Thin Film Heat Transfer Gauges," 5th ASME/JSME Thermal Engineering Joint Conference, San Diego, CA, American Society of Mechanical Engineers Paper 99-1659, 1999.

[27] Clark, J. P., Polanka, M. D., Meininger, M., and Praisner, T. J., "Validation of Heat-Flux Predictions on the Outer Air Seal of a Transonic Turbine Blade," *Journal of Turbomachinery*, Vol. 128, July 2006, pp. 589–595. doi:10.1115/1.2184351

[28] Polanka, M. D., Clark, J. P., White, A. L., and Meininger, M., "Turbine Tip and Shroud Heat Transfer and Loading, Part B: Comparisons Between Prediction and Experiment Including Unsteady Effects," American Society of Mechanical Engineers Paper GT-2003-38916, 2003.

[29] Nicholson, J. H., Forest, A. E., Oldfield, M. L. G., and Schultz, D. L., "Heat Transfer Optimized Turbine Rotor Blades—An Experimental Study Using Transient Techniques," *Journal of Engineering for Gas Turbines and Power*, Vol. 106, Jan. 1984, pp. 173–182.

[30] Mee, D., and Dickens, T., *Oxford University Engineering Laboratory Blowdown Wind Tunnel Inlet Turbulence Measurement*, Oxford Univ., Oxford, July 1987.

[31] Dorney, D. J., and Davis, R. L., "Navier–Stokes Analysis of Turbine Blade Heat Transfer and Performance," *Journal of Turbomachinery*, Vol. 114, Oct. 1992, pp. 795–806.

[32] Clark, J. P., "An Integrated Design, Analysis, and Optimization System for Turbine Airfoils," U.S. Air Force Research Lab., Wright–Patterson AFB, OH, 2004.

[33] Johnson, J. J., Clark, J. P., and Flanagan, M. J., "RANS Simulations of Turbine Vane Heat Transfer in Short Duration, Shock Tunnel Cascade Experiments," 43rd AIAA/ASME/SAE/ASEE Joint Propulsion Conference, Cincinnati, OH, AIAA Paper 2007-5000, 2007.

[34] Owen, F. K., "Transition Experiments on a Flat Plate at Subsonic and Supersonic Speeds," *AIAA Journal*, Vol. 8, No. 3, 1970, pp. 518–523.

F. Liu
Associate Editor